Robotica (2012) volume 30, pp. 405–417. © Cambridge University Press 2011
doi:10.1017/S0263574711000713

# Evaluation of 3D grasps with physical interpretations using object wrench space

Hyunhwan Jeong and Joono Cheong*

*Department of Control and Instrumentation Engineering, Korea University, Chungnam, South Korea*

(Received in Final Form: June 10, 2011; accepted June 9, 2011. First published online: July 11, 2011)

**SUMMARY**

In this paper we propose an intuitive and practical grasp quality measure for grasping 3D objects with a multi-fingered robot hand. The proposed measure takes into account the object geometries through the concept of object wrench space. Physically, the positive measure value has a meaning of the minimum single disturbance that grasp cannot resist, while the negative measure value implies the minimum necessary helping force that restores a non-force-closure grasp into a force-closure one. We show that the measure value is invariant between similar grasps and also between different torque origins. We verify the validity of the proposed measure via simulations by using computer models of a three-fingered robot hand and polygonal objects.

KEYWORDS: Grasp measure; Robot hand; Force-closure; Object wrench space.

## 1. Introduction

When grasping an object, we are often concerned about: to what amount of disturbance can the grasp resist, and which spot in the grasped object is geometrically the weakest to the disturbance. In order to answer these primary concerns, the geometry of the object must be thoughtfully incorporated into the grasp analysis. In fact, we are able to find out only a few works taking the object geometry into account for grasp analysis,[1–4] which motivated the present research in this paper.

A great number of works on grasp have been carried out for more than three decades due to its importance not only in the robotic manipulation but also in design of fixtures for manufacturing. In the earlier times of the grasp research, the fundamental issue seemed to be the examination of whether a grasp is a force-closure or not.[5–7] After that researchers tried to find a way to evaluate what finger configurations and/or contact locations yield the best performance in resisting the maximum amount of disturbance or produce a dexterous manipulation of a grasped object, which necessitated proper grasp quality measures.

Research works on grasp quality measure could be categorized by whether the grasp quality measure is dependent upon or independent of tasks. As a task-independent grasp quality measure, the maximum sphere that can be completely contained in the convex hull of grasp wrench space (GWS) was proposed by Kirkpatrick,[8] and later the meanings of the convex hulls generated by the union and the Minkowski sums of primary grasp wrenches were investigated by Ferrari and Canny.[9] Handling the friction cone was a big difficulty in analyzing grasps of 3D objects, as the friction cone in 3D space imposes strong nonlinear conditions.[10] Liu *et al.*[11] proposed a method of linearization of friction cone by approximating the friction as a polygonal pyramid with a finite number of sides.

The task-dependent (in another term, the task-oriented) grasp quality measure has not been much investigated, compared with the task-independent one. The task-dependent grasp quality measure takes into consideration particular conditions of tasks or disturbances; for example, the disturbance from gravitational force due to self-weight acts only in the downward direction to the earth frame. Li and Sastry[12] introduced the concept of task ellipsoid to select the optimal grasp by taking into account the required wrench directions. Pollard[1] defined the object wrench space (OWS) by collecting the wrenches generated by a set of force applied on the surface of the object. Later, Borst *et al.*[3] jointly utilized OWS and task ellipsoid to measure the grasp quality for discretized arbitrary 3D objects. Haschke *et al.*[13] formulated the problem of computing grasp quality measure in terms of linear matrix inequality. Strandberg and Wahlberg[4] also addressed a method of grasp quality evaluation; however, the measure value of the method is not given by a scalar value. An efficient way to determine the optimal form-closure constraints was investigated by Cornelia and Suarez[14] through an analytic procedure, an optimal or a near-optimal iterative solutions is obtained using the information of contact edges. A conventional dynamic manipulability[15] was also extended to multi-fingered grasps by considering the joint torque bounds.

More practical versions of grasp planning and control schemes are also found. A non-precision type of grasp scheme, the so-called enveloping grasp, was investigated by Salimi and Bone.[16] In their work, a grading method that analyzes the curvature pattern and effective diameter of the 3D grasped object was proposed. A blind grasping and its stabilization under gravity can be found in refs. [17, 18].

As a relatively recent research issue, the robustness of the grasp stability has been studied. Prattichizzo *et al.*[19] proposed the grasp robustness measure to cope with some uncertainties in the grasp configuration. Roa and Suarez[20] recently studied the allowable range of error for the fingertip location without loosing the force-closure condition. Platt

* Corresponding author. E-mail: jncheong@korea.ac.kr

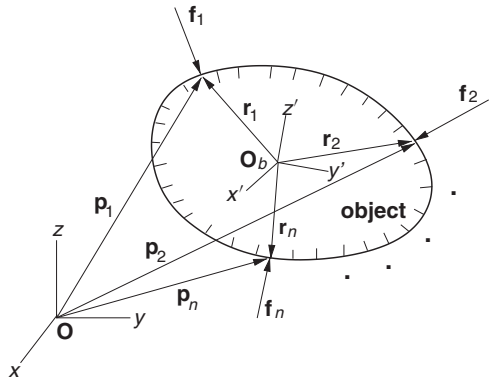


Fig. 1. Multi-point contacts for grasping a rigid body.

*et al.*[21] presented a null-space kinematic control scheme to cope with uncertainties in the real-time information of the grasped object.

In this paper we propose an enhanced grasp quality measure that conveys a clearer physical meaning and is easily interpretable. The proposed measure provides the maximum resistable disturbance in the physical force unit, together with the identification of weak spots of the object at the current grasp configuration. Mathematically, the proposed grasp quality measure is eventually formulated by means of linear optimization problems that was similarly employed in the Q-distance concept addressed in ref. [22]. The outline of the rest of the paper is as follows. Some concepts of useful wrench spaces pivotal to the current grasp analysis are defined in Section 2; after that, our grasp quality measure is detailed as the main issue in Section 3; simulation results are presented in Section 4; and finally concluding remarks are made in Section 5.

## 2. Useful Wrench Spaces

### *2.1. Absolute grasp wrench space (a-GWS)*

Consider an object that admits $n$-number of contact forces $\{\mathbf{f}_1, \mathbf{f}_2, \ldots, \mathbf{f}_n\}$ acting in the normal directions of the object surface at positions $\{\mathbf{p}_1, \mathbf{p}_2, \ldots, \mathbf{p}_n\}$, respectively, as shown in Fig. 1. Each contact force produces a torque with respect to the object's reference frame, located at the object's center of mass (CoM), such that $\boldsymbol{\tau}_i = \mathbf{r}_i \times \mathbf{f}_i$, where $\mathbf{r}_i$ is the vector from the CoM to contact point $\mathbf{p}_i$. Thus, a complete set of torques produced by all the contact forces is $\{\boldsymbol{\tau}_1, \boldsymbol{\tau}_2, \ldots, \boldsymbol{\tau}_n\}$. We assume that each robot finger contacts the object at a point with friction, so the friction cone means the appropriate region of all the admissible forces at the contact point by the robot hand. We denote $\mathrm{C}(\mathbf{p}_i)$ as the friction cone at $\mathbf{p}_i$ and $\overline{\mathrm{C}}(\mathbf{p}_i)$ as the approximated friction cone by a pyramid with $s$-number of edges. If $\mathbf{f}_{ij}$, $i = 1, 2, \ldots, n$, and $j = 1, 2, \ldots, s$, denotes the $j$th primitive force of $\overline{\mathrm{C}}(\mathbf{p}_i)$, an arbitrary force within the friction cone such that $\mathbf{f}_i^a \in \overline{\mathrm{C}}(\mathbf{p}_i)$ can be written as

$$\mathbf{f}_i^a = \sum_{j=1}^{s} \alpha_{ij} \mathbf{f}_{ij}, \tag{1}$$

with $\alpha_{ij} \geq 0$ and $\sum_{j=1}^{s} \alpha_{ij} \leq 1$. Note that the extreme case, $\sum_{j=1}^{s} \alpha_{ij} = 1$, implies that $(\mathbf{f}_i^a \cdot \mathbf{n}(\mathbf{p}_i))\mathbf{n}(\mathbf{p}_i) = \mathbf{f}_i$, where $\mathbf{n}(\mathbf{p}_i)$ represents the unit normal vector outward from the object surface at $\mathbf{p}_i$. If we define the primitive wrench, $\mathbf{w}_{ij}$, associated with $\mathbf{f}_{ij}$, as

$$\mathbf{w}_{ij} \triangleq \begin{bmatrix} \mathbf{f}_{ij} \\ \boldsymbol{\tau}_{ij} = \mathbf{r}_i \times \mathbf{f}_{ij}, \end{bmatrix}, \tag{2}$$

then the generic form of wrench that can be produced by the contact forces is written as

$$\mathbf{w} = \sum_{i=1}^{n} \sum_{j=1}^{s} \alpha_{ij} \mathbf{w}_{ij} \tag{3}$$

with $\alpha_{ij} \geq 0$ and $\sum_{j=1}^{s} \alpha_{ij} \leq 1$. The a-GWS means a space that is spanned by the primitive wrenches $\{\mathbf{w}_{11}, \mathbf{w}_{12}, \ldots, \mathbf{w}_{1s}, \ldots, \mathbf{w}_{ns}\}$ created by the physical contact forces by the exact physical scale. Since any physical robot hand due to the actuator force limit has upper bounds in producing contact forces, a-GWS from these contacts yields a case-specific absolute scale of wrench space. By combining all the primitive wrenches, we can construct a convex hull of a-GWS such that

$$\mathcal{H}_{\text{a-GWS}} \triangleq \text{ConvexHull}\left(\bigoplus_{i=1}^{n} \{\mathbf{w}_{i1}, \mathbf{w}_{i2}, \ldots, \mathbf{w}_{is}\}\right), \tag{4}$$

where $\bigoplus$ denotes the Minkowski sum of all primitive wrenches. The geometry of convex hull $\mathcal{H}_{\text{a-GWS}}$ consists of vertices, $\mathbf{v}_i, i = 1, 2, \ldots, l$, where $l \leq s^n$. For a force-closure grasp, $\mathcal{H}_{\text{a-GWS}}$ must contain zero such that $\mathbf{0} \in \mathcal{H}_{\text{a-GWS}}$, otherwise the grasp is non-force-closure. The volume of $\mathcal{H}_{\text{a-GWS}}$ indicates the size of reachable wrench space. This, in return, implies the bound of external disturbances that a given grasp can resist. Hence, an elementary grasp measure based on ref. [8]—i.e., the maximum inscribed ball measure—is expressed by

$$\mathcal{M} = \min ||\mathbf{w}||, \text{ subject to } \mathbf{w} \in \partial\mathcal{H}_{\text{a-GWS}}, \tag{5}$$

where $\partial\mathcal{H}_{\text{a-GWS}}$ denotes the boundary of $\mathcal{H}_{\text{a-GWS}}$.

### *2.2. Object wrench space (OWS)*

The grasp stability and/or robustness is always influenced by the shapes of grasped objects. Thus, it is natural to incorporate the surface geometry of the objects into the grasp measure through some way in order to achieve a result faithful to physical sense. In light of this aspect, measure $\mathcal{M}$ in Eq. (5), for instance, computed without considering the overall geometry of the object may not be suitable to reflect the real physics.

One prominent way to incorporate the geometry of object into the grasp quality measure is to use the concept of OWS, which is a vector space spanned by wrenches generated by a set of distributed linear forces on the surface of a grasped object. The set of distributed forces approximates all the possible external disturbances imparted on the object. Although the concept of OWS was first defined in ref. [1], a rigorous use of OWS in defining a task-oriented grasp quality

https://doi.org/10.1017/S0263574711000713 Published online by Cambridge University Press

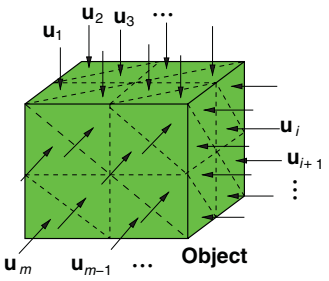


Fig. 2. (Colour online) A distribution of forces that produce OWS for a 3D polygonal object.

measure was done by Borst *et al.*[3] As addressed in ref. [3], the generic form of the object wrench is

$$\mathbf{w} = \sum_{i=1}^{m} \gamma_i \mathbf{w}_i, \quad \gamma_i \geq 0, \quad \text{and} \quad \sum_{i=1}^{m} \gamma_i = 1, \tag{6}$$

where $m$ is the number of corners of the polygonal object, and $\mathbf{w}_i$ denotes the wrench produced by the force, $\mathbf{u}_i$, of the unit magnitude within the friction cone, acting on the $i$th corner, satisfying

$$||\mathbf{u}_i - \mathbf{u}_i \cdot \mathbf{n}_i|| \leq \mu ||\mathbf{u}_i \cdot \mathbf{n}_i||,$$

where $\mathbf{n}_i$ and $\mu$, respectively, denote the normal direction of the $i$th facet on the discretized object and the friction coefficient. The wrench in Eq. (6), which spans OWS, is generated by any combination of forces whose $L_1$ norm (i.e., sum of magnitudes) is 1, so as to normalize the effect of the disturbance. The problem about this OWS is that there can be infinite choices of $\mathbf{u}_i$ even at a single corner, which complicates constructing of convex hull of OWS. In order to reduce the complexity, in ref. [3], a sampling method for choosing $\mathbf{u}_i$s was employed, and, from this, an ellipsoid of OWS was created that is an approximate of the exact convex hull of OWS; this was similar to the task ellipsoid concept addressed in ref. [12]. However, the approach in ref. [3] still has some drawbacks, such as (i) the number of samples should be sufficiently large, while it is not clear how many samples are sufficient, (ii) even if a sufficient number of samples is employed, the convex hull of OWS is, after all, approximated by an ellipsoid, with which an asymmetric object may not work well, and (iii) while the measure value directly indicates the maximum allowable wrench in $\mathbb{R}^6$, the measure may not be relevant to admissible disturbance forces on the object due to the use of approximate ellipsoid.

Inspired by this observation, we propose a modified OWS that is generated by a set of distributed surface forces acting only normal to the surface as shown in Fig. 2. These surface forces represent a set of all possible disturbances acting on the surface normal. Ignoring the tangential components in the surface forces effectively is equivalent to assuming that the surface is frictionless. The reason for such a deliberated assumption is as follows: Under the condition that we realistically cannot and may not have to take into account all disturbances for evaluating a grasp quality, it would make more sense to limit the disturbances to be those of the most probable ones, which must be the normal forces on the surface. Due to this setup, the OWS can be described by a finite number of wrenches that is sufficient to capture the overall characteristic of the disturbances, and, as a consequence, a correct shape of convex hull for the OWS is obtained. Besides, such a setup allows us to identify the most fatal spot on the object, along with the associated disturbance force. This aspect makes the grasp evaluation more useful in practice and conveys a clearer physical meaning (we shall discuss this issue in Section 3.3).

In order to define the proposed OWS mathematically, let us consider a polygonal object with a large number of facets on the surface. For an object with $m$-numbered surface facets, the OWS is created by a set of elementary wrenches,

$$\mathbf{z}_k = \begin{bmatrix} \mathbf{u}_k \\ \mathbf{l}_k \times \mathbf{u}_k, \end{bmatrix}, \quad k = 1, 2, \ldots, m, \tag{7}$$

where $\mathbf{l}_k$, $\mathbf{u}_k$, and $\mathbf{z}_k$, respectively, denote the vector from the origin of the object frame (or the center of mass) to the $k$th facet, the unit normal surface force at $\mathbf{l}_k$, and the wrench produced by $\mathbf{u}_k$. With the set of elementary wrenches, the convex hull of OWS is created by the convex combination of $\mathbf{z}_i$s such that

$$\mathcal{H}_{\text{OWS}} \triangleq \text{ConvexHull}\left(\{\mathbf{z}_1, \mathbf{z}_2, \ldots, \mathbf{z}_m\}\right). \tag{8}$$

This convex geometry is ultimately composed of vertices $\bar{\mathbf{z}}_j$, $j = 1, 2, \ldots, d \leq m$, belonging to a set of elementary wrenches in Eq. (7). Please remind that $\mathcal{H}_{\text{a-GWS}}$, different from $\mathcal{H}_{\text{OWS}}$, was constructed by the Minkowski sum.

Note that $\mathcal{H}_{\text{OWS}}$ is an exact wrench set that describes all the possible external disturbances bounded by unit norm, in the sense that all the $m$-number of elementary wrenches are involved in constructing the convex hull. It accommodates the information on the shape of the polygon geometry; objects with different surface geometries have different shapes of $\mathcal{H}_{\text{OWS}}$. Hence, the shape of the convex hull of OWS may be regarded as an object characteristic. It is possible that $\mathcal{H}_{\text{OWS}}$ is computed off-line using the CAD information of the object geometry. For similar objects with different geometric scales, the shapes of $\mathcal{H}_{\text{OWS}}$ are very alike, except the scale difference in the $\tau$-axes. For instance, for a 2D object with the unit square shape and a similar one scaled by 2 as shown in Fig. 3(a) and (b), respectively, the $\mathcal{H}_{\text{OWS}}$s differ only in the $\tau_z$ axis, while the projections of the convex hulls onto $f_x$–$f_y$ plane are identical, as shown in Figs. 3(c) and (d).

It is also noteworthy that $\mathcal{H}_{\text{OWS}}$ for any object possesses $\mathbf{0}$ as an interior point without regard to the shape of an object and coordinate frames. This is because the surface of an object in 3D space is closed, and thus any force applied on the surface of the object has some combination of surface forces that result in equilibrium.

Inverting the object wrenches, we obtain another convex hull as

$$\overline{\mathcal{H}}_{\text{OWS}} \triangleq \text{ConvexHull}\left(\{-\mathbf{z}_1, -\mathbf{z}_2, \ldots, -\mathbf{z}_m\}\right),$$

which is point symmetric with $\mathcal{H}_{\text{OWS}}$ about the origin but shares most of the properties of $\mathcal{H}_{\text{OWS}}$. This reflected convex

https://doi.org/10.1017/S0263574711000713 Published online by Cambridge University Press

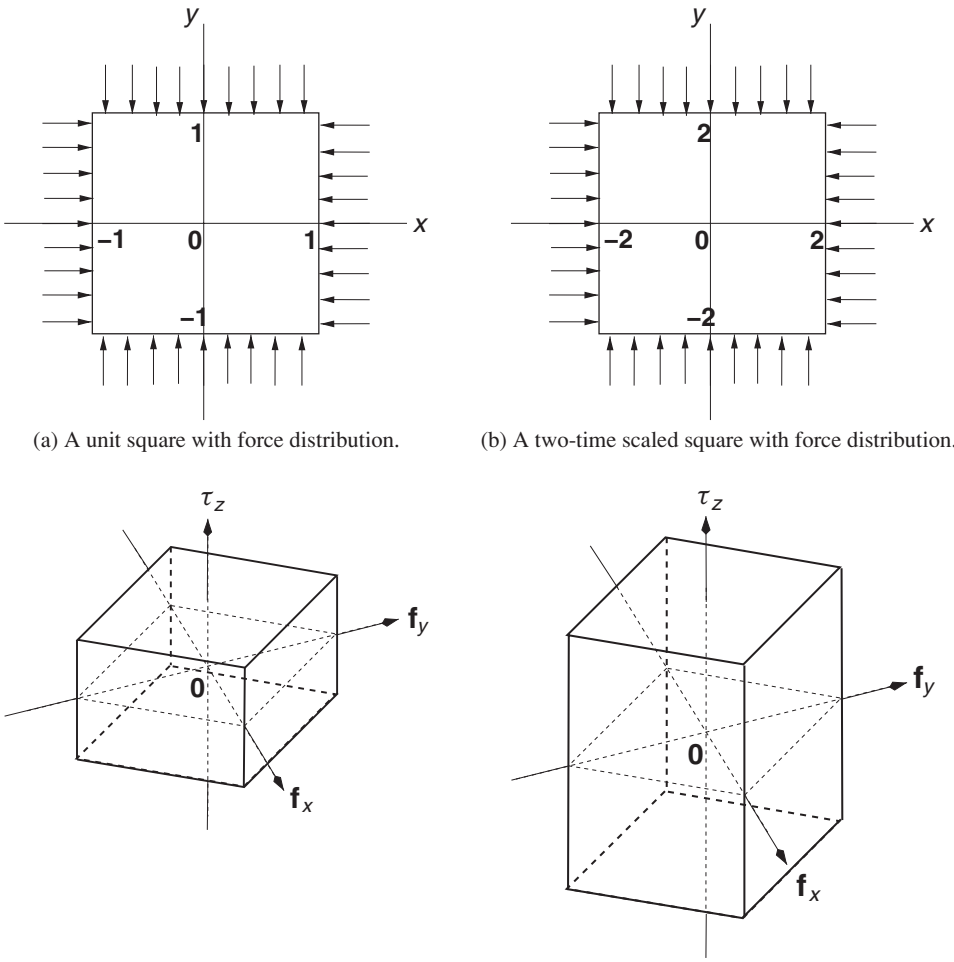


(a) A unit square with force distribution.

(b) A two-time scaled square with force distribution.

(c) Convex hull of OWS for the unit square.

(d) Convex hull of OWS for the scaled square.

Fig. 3. 2D square objects and their object wrench spaces.

hull is useful for treating the object wrenches as the external input source that must be statically equilibrated by the grasp wrenches.

## 3. Grasp Quality Measure

### *3.1. Maximum contact force*

Since the magnitude of the contact force determines the size of $\mathcal{H}_{\text{a-GWS}}$, it must be the first step to determine at each fingertip the maximum magnitude of the contact force that a real finger, driven by actuators with limited torque bounds, can impart at a given configuration. In order to solve this problem, consider the following static force–torque relation:

$$\mathbf{J}_i^T(\boldsymbol{\theta}_i)\mathbf{f}_i^e = \mathbf{T}_i, \quad i = 1, 2, \ldots, n, \tag{9}$$

where $\mathbf{J}_i(\boldsymbol{\theta}_i) \in \mathbb{R}^{n_x \times n_{qi}}$, $\mathbf{f}_i^e \in \mathbb{R}^{n_x}$, $\mathbf{T}_i \in \mathbb{R}^{n_{qi}}$, and $\boldsymbol{\theta}_i \in \mathbb{R}^{n_{qi}}$, respectively, denote the finger Jacobian matrix, the force at the finger tip, the joint torque, and the joint angle with $n_{qi}$ and $n_x$ being the number of joints and the dimension of workspace, all associated with the $i$th articulated finger. From this setting, we need to solve the following optimization:

$$\text{Maximize} \; -\mathbf{n}(\mathbf{p}_i)\cdot\mathbf{f}_i^e, \; \text{subject to} \begin{Bmatrix} \mathbf{n}(\mathbf{p}_i)\left[(\mathbf{n}(\mathbf{p}_i)\cdot\mathbf{f}_i^e\right] = \mathbf{f}_i^e \\ \mathbf{J}_i^T(\boldsymbol{\theta}_i)\mathbf{f}_i^e = \mathbf{T}_i \\ -\beta_{ij} \le T_{ij} \le \beta_{ij} \end{Bmatrix},$$
$$\text{for } i = 1, 2, \ldots, n, \; j = 1, 2, \ldots, n_{qi}, \tag{10}$$

where $\mathbf{p}_i$ is the contact point coincident with the $i$th finger tip position, $T_{ij}$ represents the joint torque, and $\beta_{ij} > 0$ is a constant joint torque limit, associated with the $j$th joint in the $i$th finger. In the above equation, the first equality condition constrains that $\mathbf{f}_i^e$ remains normal to the surface, otherwise the fingertip force could be slanted from the normal vector, and, thus, the active tangential component of fingertip force would work as an adverse disturbance, which causes a loss of some reachable wrenches in a-GWS. As shown in Fig. 4, as the direction of contact force approaches the boundary of the friction cone, the margin to resist the disturbance in the tangential direction becomes reduced. The inequality condition in Eq. (10) simply restricts the limit of joint torque. Once Eq. (10) is solved through some linear programing, the maximum normal contact force, $\mathbf{f}_i^{e*}$, becomes available and

https://doi.org/10.1017/S0263574711000713 Published online by Cambridge University Press

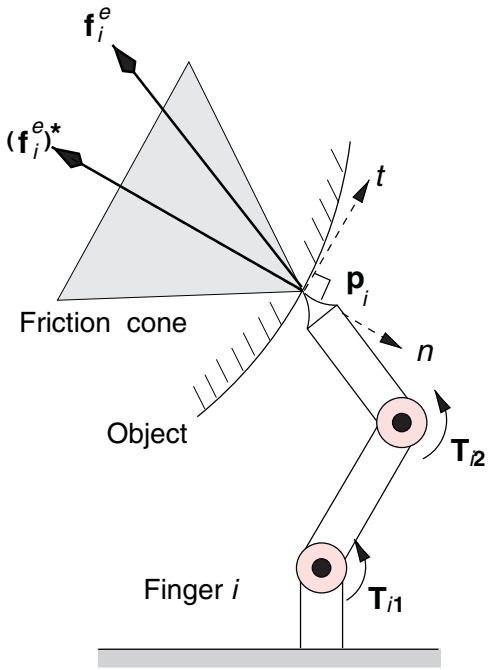


Fig. 4. (Colour online) Schematic of the direction of contact force by a two-link robot finger.

works as a contact force that generates primitive wrenches of a-GWS in Eq. (2).

### 3.2. *Proposed grasp quality measure*

Our grasp quality measure is designed to find the minimum (or maximum) force equilibrium condition through a geometrical relation between convex hulls of a-GWS and OWS. Conceptually, our grasp measure is defined, through the convex geometrical relation, as (i) the maximum scale of $\overline{\mathcal{H}}_{\text{OWS}}$ that is completely contained in $\mathcal{H}_{\text{a-GWS}}$ when $\mathbf{0} \in \mathcal{H}_{\text{a-GWS}}$, and (ii) negative of the minimum scale of $\overline{\mathcal{H}}_{\text{OWS}}$ that begins to touch $\mathcal{H}_{\text{a-GWS}}$ when $\mathbf{0} \notin \mathcal{H}_{\text{a-GWS}}$. Figs. 5 (a) and (b) show the schematic diagrams of the measure for case (i) and case (ii), respectively.

Mathematically, the proposed concept of grasp quality measure is formulated as follows:

(i) $\mathbf{0} \in \mathcal{H}_{\text{a-GWS}}$ (force-closure):

$$\mathcal{M} = \min_{k=1,2,\ldots,d} \max \ \rho_k \tag{11}$$

$$\text{subject to} \left\{ \begin{array}{l} \rho_k(-\bar{\mathbf{z}}_k) = \sum_{j=1}^{l} \lambda_j \mathbf{v}_j \\ \sum_{j=1}^{l} \lambda_j = 1 \\ \rho_k \geq 0, \lambda_j \geq 0. \end{array} \right\}. \tag{12}$$

(ii) $\mathbf{0} \notin \mathcal{H}_{\text{a-GWS}}$ (non-force-closure):

$$\mathcal{M} = -\min \sum_{k=1}^{d} \rho_k \tag{13}$$

$$\text{subject to} \left\{ \begin{array}{l} \sum_{k=1}^{d} \rho_k(-\bar{\mathbf{z}}_k) = \sum_{j=1}^{l} \lambda_j \mathbf{v}_j \\ \sum_{j=1}^{l} \lambda_j = 1 \\ \rho_k \geq 0, \lambda_j \geq 0. \end{array} \right\}. \tag{14}$$

The solution for this problem is found exactly when the scaled $\overline{\mathcal{H}}_{\text{OWS}}$ first touches the boundary of $\mathcal{H}_{\text{a-GWS}}$. By the formulations, a positive value of $\mathcal{M}$ represents a force-closure grasp, while a negative value of $\mathcal{M}$ means a non-force-closure grasp. For a marginal grasp case, $\mathcal{M}$ is zero. The grasp measure varies continuously under a smooth change of a grasp condition such as the gradual change of contact points or finger configurations, without regard to whether a grasp is a force-closure or not, assuming the surface of the object is smooth. Furthermore, for a force-closure grasp, the amount of measure value tells how much the current grasp can support external forces whereas for a non-force-closure grasp the measure value indicates the amount of required assistive external force that recovers the current grasp into a force-closure. Thus, the proposed measure can effectively evaluate a grasp's quality by taking into account the object geometry.

As shown in Eqs. (11)–(14), the measure is computed with the object wrenches inverted to the opposite directions, i.e., $-\bar{\mathbf{z}}_k$. This is equivalent to using the reflected OWS, $\overline{\mathcal{H}}_{\text{OWS}}$, as shown in schematic in Fig. 5. The fundamental reason to use the inverted object wrench is to formulate the definition of

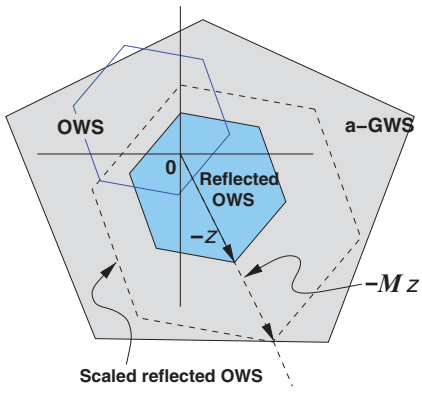


(a) Measure for a force-closure grasp ($\mathcal{M} > 0$).

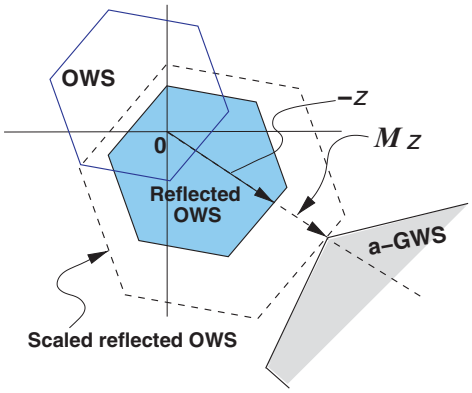


(b) Measure for a non-force-closure grasp ($\mathcal{M} < 0$).

Fig. 5. (Colour online) Schematic of computing the grasp quality measure using a-GWS and OWS.

https://doi.org/10.1017/S0263574711000713 Published online by Cambridge University Press

the measure consistent with the physics law of equilibrium between the contact forces and the disturbances. In fact, the first equality constraint in Eqs. (12) and (14) represents the static equilibrium condition between the disturbance wrench and its counter-balancing wrench by contact forces.

There are a couple of invariant properties of the proposed measure, which is desirable in the sense of intuitiveness. First, the proposed measure is invariant under different torque origins. According to the statics, a condition for static force equilibrium must remain the same regardless of the torque origin. The proposed measure formulated in Eqs. (11) and (12), as mentioned before, is a static equilibrium problem that seeks the solvable extreme case. Hence, the resulting solution would not vary even if a different torque origin is used. The same principle applies to the non-force-closure case of the proposed measure formulated in Eqs. (13) and (14). Second, the proposed measure is invariant between similar grasps, where the similar grasps refer to grasps that can be reduced to an identical grasp if the grasped objects with the contact configurations are scaled appropriately. Since the proposed measure is determined by the relative ratio between the convex hulls of a-GWS and OWS, a simultaneous scale-increment or scale-decrement of the two convex geometries does not make any difference to the proposed measure. This situation happens when we evaluate grasps with scale similar objects. These two invariance properties reflect man's general intuition for grasping as discussed in ref. [3].

We should remark that the proposed grasp quality measure has a similarity with Q-distance measure proposed by Zhu and Wang.[22] The Q-distance measure is mathematically defined by the $L_2$ distance between a test polyhedral set, the so-called Q, and the conventional convex hull of GWS. The differences between our grasp measure and the Q-distance are as follows: (1) The physical meaning of the measure by Q-distance is ambiguous since the set Q is an abstract set, although the Q-distance is generically defined in mathematical sense. On the contrary, our measure exhibits a clear and concrete physical meaning by jointly using the convex hulls of the Minkowski sum-based a-GWS and the union-based reflected OWS. (2) The proposed measure is invariant under torque origins and shows scale similarity, while the Q-distance measure is generally not. (3) Moreover, the wrench direction to the minimum Q-distance does not tell anything, while the wrench direction to the minimum of the proposed measure is associated with the most fatal spot on the object surface to the disturbance, which will be detailed in the next subsection.

### *3.3. Physical meaning of grasp quality measure*

According to the definition of the proposed grasp quality measure, measure $\mathcal{M}$ for a force-closure grasp implies the maximum scale of $\overline{\mathcal{H}}_{\text{OWS}}$ contained completely in $\mathcal{H}_{\text{a-GWS}}$. Since $\overline{\mathcal{H}}_{\text{OWS}}$ is constructed by the wrenches from the distributed unitary surface forces, the scaled $\overline{\mathcal{H}}_{\text{OWS}}$ by $\mathcal{M}$ amount is equivalent to the convex hull generated by the wrenches from the distributed surface forces scaled by the same amount. Therefore, $\mathcal{M}$ is physically the maximum magnitude of an arbitrary external surface force that the robot hand can always resist. Furthermore, $\overline{\mathbf{z}}^*$, associated with the solution of Eqs. (11) and (12), satisfying $\partial\mathcal{H}_{\text{a-GWS}} = -\mathcal{M}\overline{\mathbf{z}}^*$, denotes, to the current grasp, the weakest directional wrench produced by a single unitary surface force, $\overline{\mathbf{u}}^*$. Since each surface force is associated with the location of action on the object surface, we are able to identify the most fatal spot where $\overline{\mathbf{u}}^*$ is applied. Ultimately, the proposed measure is completely characterized by the surface force, $\mathcal{M}\overline{\mathbf{u}}^*$, with the associated facet in the polygonal surface. This single force representation of the grasp quality measure is attractive due to its intuitiveness and conciseness.

Compared with the case of the force-closure grasp, the measure value in a non-force-closure grasp is the minimum scale of $\overline{\mathcal{H}}_{\text{OWS}}$ that begins to intersect with $\mathcal{H}_{\text{a-GWS}}$. This scale value implies the minimum amount (in $L_1$ norm sense) of helping forces, exerted on the object surface that, if added to a-GWS, stretches the boundary of a-GWS to pass through the origin such that

$$\mathbf{0} \in \partial\mathcal{H}^*_{\text{a-GWS}},$$

where

$$\mathcal{H}^*_{\text{a-GWS}} \triangleq \text{ConvexHull}\left(\mathcal{H}_{\text{a-GWS}} \bigoplus \left\{\sum_{k=1}^{d} \rho_k^* \overline{\mathbf{z}}_k^*\right\}\right),$$

where $\rho_k^*$ and $\overline{\mathbf{z}}_k^*$ denote the solution of Eqs. (13) and (14). Physically speaking, the solution wrench, $\sum_{k=1}^{d} \rho_k^* \overline{\mathbf{z}}_k^*$, implies the required minimum external wrench that restores a non-force-closure grasp into a force-closure grasp. Unfortunately, as shown in Fig. 5(b), the first intersection does not necessarily occur at a vertex of the scaled $\overline{\mathcal{H}}_{\text{OWS}}$. The measure value in the non-force-closure grasp, hence, is not characterized by only a single representative force on the object surface. If the first intersection occurs at a face, the measure value is obtained by a magnitude sum of a particular distribution of surface forces such that

$$\{\rho_1^* \overline{\mathbf{u}}_1,\ \rho_2^* \overline{\mathbf{u}}_2, \ldots, \rho_d^* \overline{\mathbf{u}}_d\}_{\text{surface}} \tag{15}$$

where $\overline{\mathbf{u}}_k, k = 1, 2, \ldots, d$ is the unitary surface force that generates wrench $\overline{\mathbf{z}}_k$.

## 4. Simulation Study

In this section, we present results of numerical simulation showing the validity and performance of the proposed measure. First, simple 2D grasp examples, intending for conveying intuitive understanding and verification of the measure, are illustrated, followed by 3D grasp examples with a three-fingered robot hand. The simulator for 3D grasp examples is designed for a arm–hand combined manipulation through a 7-DOF manipulator holding a three-fingered robot hand at the end. A screen capture of our 3D simulator is shown in Fig. 6.

The detailed simulation procedures for general 3D grasp examples are summarized as follows.

*Step 1.* First, a target polygonal object to be grasped is loaded, followed by a generation of OWS and its convex hull. Since OWS of an object and the

https://doi.org/10.1017/S0263574711000713 Published online by Cambridge University Press

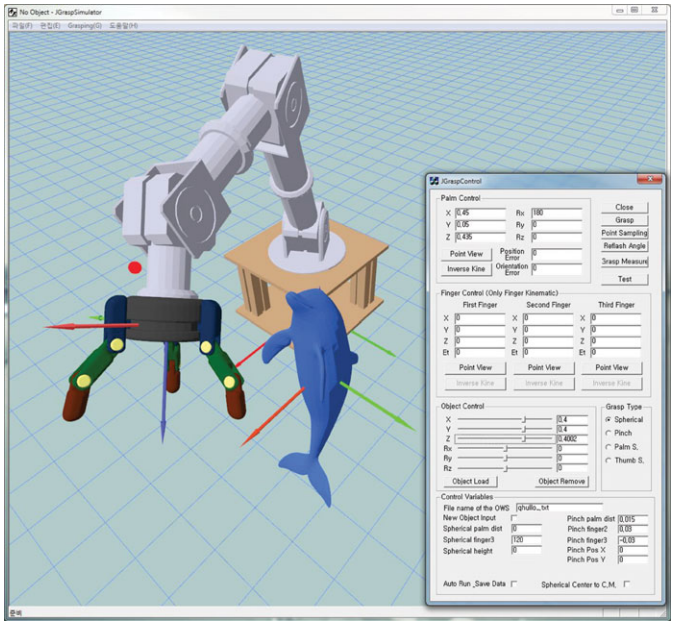

Fig. 6. (Colour online) Screen capture of grasp simulator. A three-fingered hand on a 7-DOF manipulator grasps 3D polygonal objects.

corresponding convex hull can be computed off-line and stored for later use, this time-consuming step may be omitted in the on-line implementation.

*Step 2*. The palm of the robot hand is moved to the assigned position and orientation with respect to the object frame, and the contact points are sampled in accordance with the grasp taxonomy[23] that suits for grasping the target object.

*Step 3*. The inverse kinematics routine is executed so as to determine the joint configuration of each finger to place the fingertip onto the sampled contact point. Subsequently, by employing the determined joint configuration, the maximum normal contact force is computed through Eq. (10).

*Step 4*. Now, having all information of contact points and the contact forces, we create a-GWS and its convex hull.

*Step 5*. Using the convex hulls of OWS and a-GWS, we obtain the measure value by solving Eqs. (11)–(14).

### *4.1. 2D grasp examples*

In this subsection, the properties and strength of the proposed measure are demonstrated through 2D grasp examples. We assume that the contacts occur at two opposite sides with friction. Each maximum contact force is set to $1\,N$, with friction coefficient, $\mu = 0.3$. Note that in 2D grasps we do not consider the effect of finger configurations.

The first 2D grasp example is for elucidating whether the object shape affects the grasp quality under a specified grasp measure. Our grasp measure is compared with the classical inscribed ball measure. As shown in Fig. 7, two different objects are selected for the test; one is of letter C shape and the other is of letter half C shape. Both objects have their origins of the reference frames outside the bodies. The measure values are computed by varying contact 1 to the left from an initial state that exhibits an exact opposition with contact 2. As shown in Fig. 8(a), the measure value based on our grasp quality measure decreases gradually as contact 1 moves left from the opposition axis. Note that the measure value, having the unit Newton (N), physically implies the weakest normal external force that cannot be resisted by the grasp. Since our grasp quality measure takes into account the geometric shapes of the objects through their OWS, the measure values between the objects of letter C and half C differ. To be more precise, measure values for the object of letter C show smaller values than the other. This means that the grasp for the object of letter C can resist less amount of external force than for the other case.

On the contrary, the inscribed ball measure shows exactly the same measure values for both objects. As the inscribed ball measure is affected only by the relative configuration between contact points, changing the object geometry would not directly influence the measure value. In the inscribed ball measure, the non-force-closure grasps are not defined well; thus, the measure values have been only computed for the force-closure grasps. However, the decision whether a grasp is force-closure or not must be determined correctly via any grasp measure. As shown in Fig. 8, the locations of contact 1 where measure values become exactly zero are the same under both grasp measures; thus, it is certain that both grasp measures can correctly recognize the force-closure condition.

In Fig. 8(a) we notice that the slopes of the graphs in the regions of force-closure and non-force-closure are different. This is because the physical meanings and the computed conditions between the positive measure and the negative

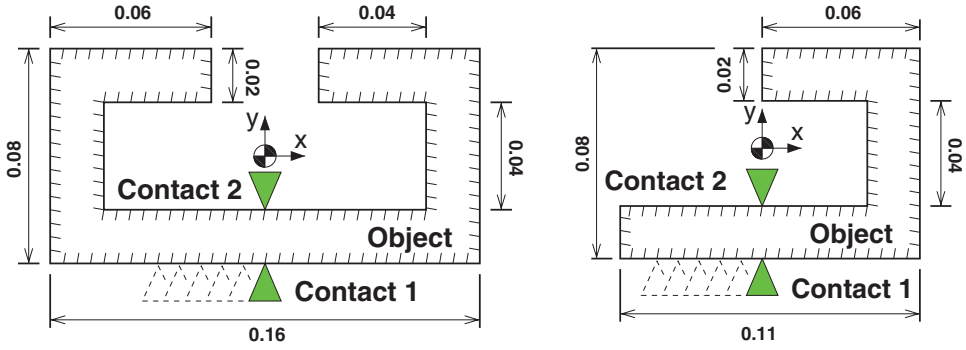


(a) Object of letter C shape. (b) Object of letter half C shape.

Fig. 7. (Colour online) Geometric shapes and dimensions of 2D objects and the contact configurations.

https://doi.org/10.1017/S0263574711000713 Published online by Cambridge University Press

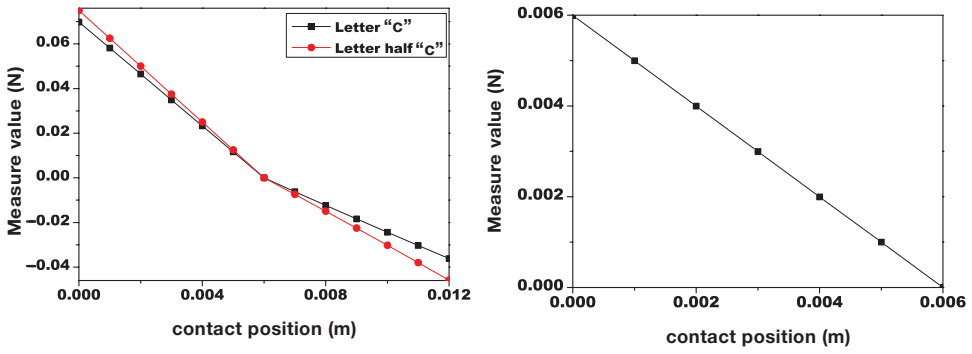


(a) Proposed grasp quality measure. (b) Inscribed ball measure.

Fig. 8. (Colour online) Simulation results of grasping objects of letter C and half C.

measure are different from each other. However, this slope change occurs only once and does not give much impact for grasp analysis, planning, and/or synthesis.

Another notable property of our grasp measure is that it has nothing to do with the torque origin, while some measures, including the inscribed ball measure, inscribed ball with torque scaling measure, and volume of grasp wrench space measure, are dependent upon it. To illustrate this, we change the torque origin (and the reference frame) of the object of letter C to another location, as shown in Fig. 9(a), and compare the measure values. As shown in Fig. 9(b), the measure values based on our grasp quality measure, even with a different torque origin, remain the same as those in Fig. 8(a). This property of our grasp quality measure is agreeing with human intuition, for which the torque origin is an artificial conception that has nothing to do with human grasping.

Next example is to demonstrate the invariant property of the proposed measure between similar grasps. For this, the size of the object of letter C as shown in Fig. 7(a) is scaled up and down, while its geometrical shape remains similar. Then, by gradually moving contact 1 to the left from the initial opposition state, our grasp quality measures are computed. As shown in Fig. 10, we obtain identical measure values for the contact locations where exact grasp similarity is satisfied. That is, the objects of 0.5, 1.0, 1.5, and 2.0 times of original scale yields the same measure values (i.e., 0.025 N) when

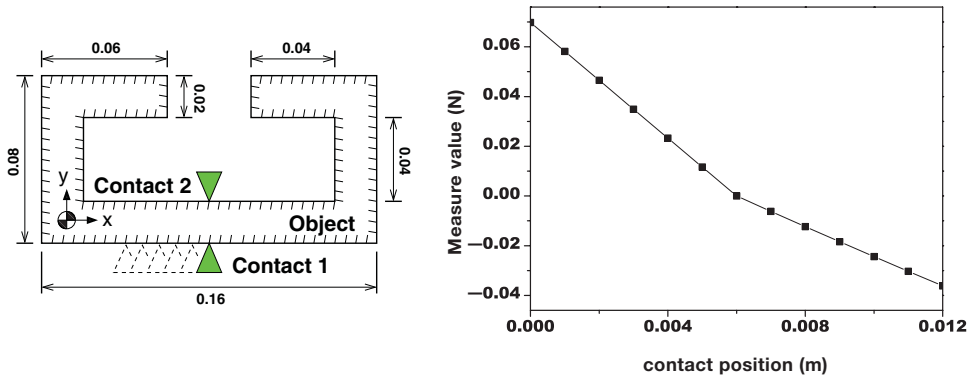


(a) Object of letter C with a different reference frame. (b) Result of the proposed grasp quality measure.

Fig. 9. (Colour online) Simulation results of grasping an object of letter C with a different reference frame.

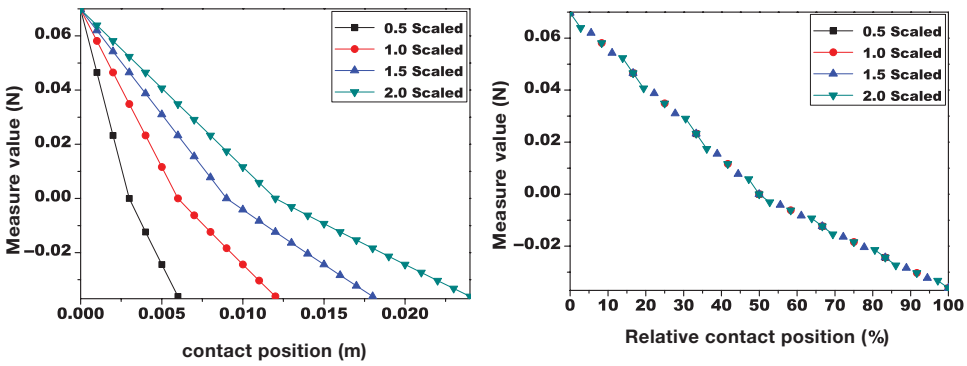


(a) Measure values for scaled objects. (b) Measure values for scaled objects after normalization.

Fig. 10. (Colour online) Comparison of measure values based on our grasp quality measure for grasping objects of letter C shape with different scales.

https://doi.org/10.1017/S0263574711000713 Published online by Cambridge University Press

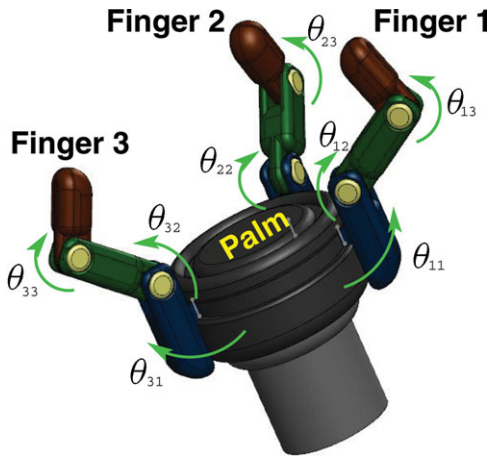


Fig. 11. (Colour online) Schematic of the three-fingered hand used for simulation. Since each finger has three joints, placing a fingertip to a designated 3D contact point is possible.

contact 1 is placed at 2.5 mm, 5 mm, 7.5 mm, and 10 mm, to the left, respectively, for which the considered grasps become similar grasps. For the rest of other contact locations, the results show that the measure values are identical between the scaled objects as long as the contact locations are consistently configured with respect to the scaled objects. Fig. 10(b), obtained after normalizing the contact locations, clearly verifies the scale-invariant property of the proposed grasp measure. In addition, if we proportionally adjust the maximum contact forces as the object size varies, then the measure value will accordingly vary, showing exactly the same proportion.

### *4.2. 3D simulation results*

Three illustrative 3D grasp examples are shown in this subsection. The first one is intended to show the validity of the grasp quality measure for grasping 3D objects, the second one shows the visualization of grasp measure exactly on the surface of the objects through the color gradient, and the last one is to demonstrate the effect of finger configurations to the grasp quality measure. For 3D grasp simulations, a three-fingered robot hand having a total of 9 DOFs—3 DOFs for each finger—is used as shown in Fig. 11. The torque limit of each actuator in the robot hand is identically set to be $-1\ Nm \leq T_{ij} \leq 1\ Nm$, where $i = 1, 2, 3$ and $j = 1, 2, 3$, for simplicity. The maximum contact force is computed by Eq. (10), and the friction coefficient is set to be $\mu = 0.3$.

In this simulation, we test the grasp quality measures by grasping four 3D objects that are having the shapes of a dolphin, rook, boomerang, and lion. We consider contact points and finger configurations as variables. As shown in Fig. 12(a) and (d), a dolphin and a lion are grasped using

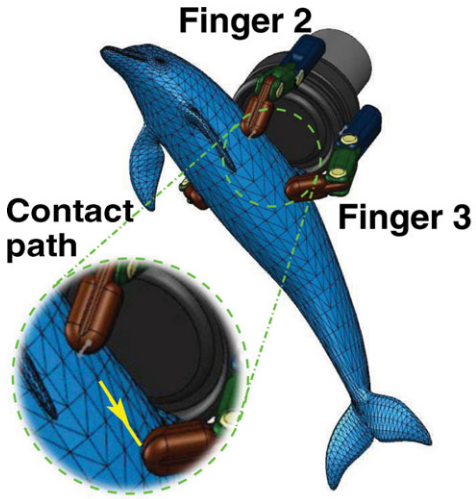


(a) Pinch grasp for a dolphin shape.

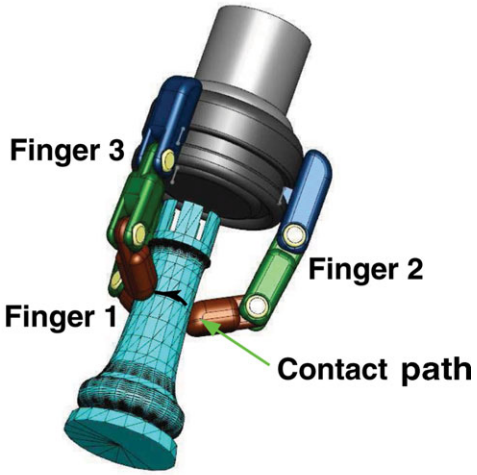


(b) Spherical grasp for a rook shape.

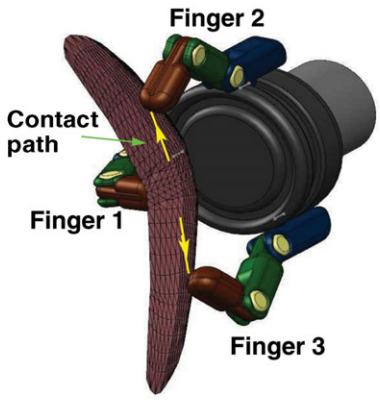


(c) Pinch grasp for a boomerang shape.

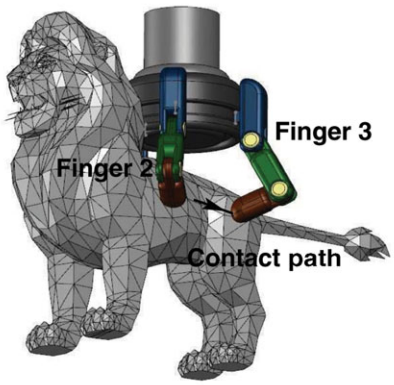


(d) Pinch grasp for a lion shape.

Fig. 12. (Colour online) Schematics of grasps for various 3D polygonal objects.

https://doi.org/10.1017/S0263574711000713 Published online by Cambridge University Press

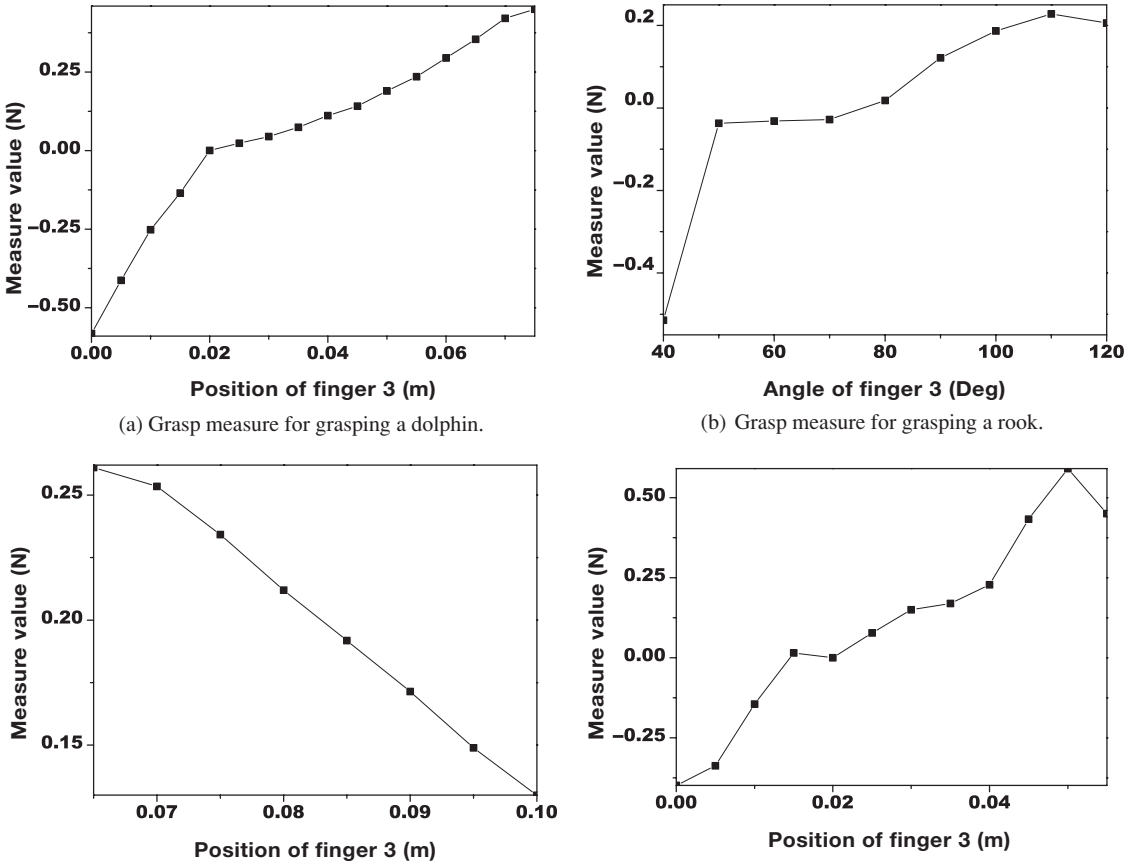


(a) Grasp measure for grasping a dolphin.

(b) Grasp measure for grasping a rook.

(c) Grasp measure for grasping a boomerang.

(d) Grasp measure for grasping a lion.

Fig. 13. Grasp quality measures for grasping 3D objects.

the pinch method, where only the contact point by finger 3 is gradually varying, starting from the overlapped position with finger 2 to the final position shown in the figure. Next, as shown in Fig. 12(b), a rook is grasped through the spherical method, where three fingers, approaching from the top, are symmetrically grasping the object. In this test, while fixing fingers 1 and 2, we gradually rotate finger 3 from the overlapped position with finger 2 to the final symmetric configuration as shown in the figure. Figure 12(c) shows grasping a boomerang using the pinch method. In this case, the contact positions of fingers 2 and 3 are gradually moving away into opposite direction.

As shown in Fig. 13, measure values for all the cases are continuously varying with different contact positions. Since the facets on the surfaces of rook and lion are rather coarse and uneven, the graphs for grasp quality measure are little rugged. These measure values represent the physical force quantity in Newton. In particular, the measure values for the force-closure cases imply single forces at the most fatal locations on the object surface.

Figure 14 shows resistibility of the current grasp configuration by the blue–red color gradient on the surface while grasping four objects. For this, we compute the maximum resistable external force acting at each vertex on the object surface, and normalize it in order to map into the blue–red color gradient smoothly. In these figures, the surface region having red color is structurally weak for external forces, and the other surface region having blue color is strong for external forces. The most reddish spot corresponds to the most fatal location under the external force. (In the figure, arrows indicate the most fatal locations of the four tested objects.)

The computation time for obtaining the measures in these cases ranges from several seconds to tens of seconds with a Core I7 Intel processor, so the real-time implementation of the proposed measure would not be possible. However, the currently popular multi-core-based parallel processing technique is promising for a substantial reduction of computation time. Commercially available CPUs are composed of several sub-cores that can be programed for parallel computation. Even more, a normal Graphical Processing Unit (GPU) of a graphic card is composed of more than a thousand stream cores that can be also programed to perform general floating-point computations in parallel. Thus, technically we can take advantage of such a new way of parallel processing for reducing the computation time and thereby enabling real-time implementation of the proposed measure.

Finally, the effect of finger configuration to the grasp quality measure is investigated. With identical contact points on an identical object, we change the relative positions of the palm and the object so as to elicit a change in finger configurations. The maximum contact forces at fingertips generally increase as the finger configurations become more bent due to the reduction of the distance between the palm and the object. This observation agrees with the behavior of human hand. As a set of larger contact forces produces

https://doi.org/10.1017/S0263574711000713 Published online by Cambridge University Press

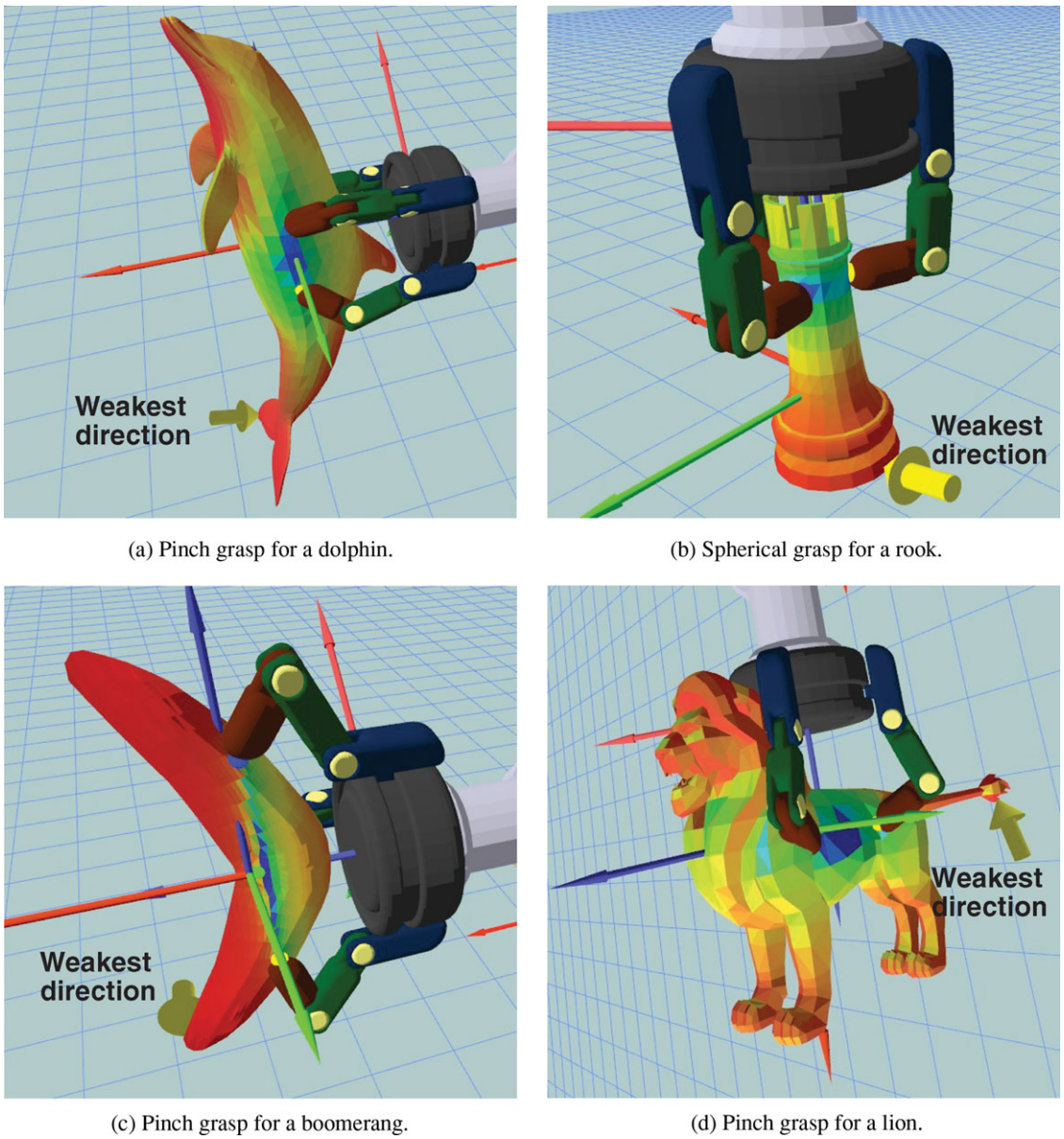


(a) Pinch grasp for a dolphin.

(b) Spherical grasp for a rook.

(c) Pinch grasp for a boomerang.

(d) Pinch grasp for a lion.

Fig. 14. (Colour online) Blue–red color gradient of resistable external forces for given grasp configurations. Blue color implies good resistibility whereas red color implies bad resistibility.

a bigger convex hull of a-GWS, it is natural that the grasp resistibility would be enhanced. Please refer to Fig. 15 for detailed numerical results.

## 5. Conclusion

In this paper we proposed a computational method to evaluate grasp quality using OWS and a-GWS, leading to a physically meaningful measure value. We suggested a way to create a suitable OWS and a-GWS, through which we simplified and made more useful the conventional OWS and GWS. Ultimately, a mathematical closed-form formulation of the grasp quality measure for both force-closure and non-force-closure grasps was established as linear optimization problems. We show that the measure value, for a force-closure grasp, directly implies the maximum amount of a single linear disturbance that the robot hand can resist whereas, for a non-force-closure grasp, it implies the required minimum linear force to be needed in order to restore the grasp to be a force-closure. The proposed measure is invariant under torque origins. The proposed measure is also invariant between similar grasps. We verified the validity of the proposed grasp quality measure through numerical simulations. We believe that due to its practicality and systematic nature the proposed measure can be used in broad range of applications for grasp analysis, planning, and grasp synthesis.

## Acknowledgment

This research was supported, in part, by Basic Science Research Program through the National Research Foundation of Korea (NRF) funded by the Ministry of Education, Science and Technology (2009-0075730), by the Converging Research Center Program funded by the Ministry of Education, Science and Technology (2010K001163), by the Intelligent Robotics Development Program, one of the 21st Century Frontier R&D Programs, and by the center for Autonomous Manipulation under Human Resources

https://doi.org/10.1017/S0263574711000713 Published online by Cambridge University Press

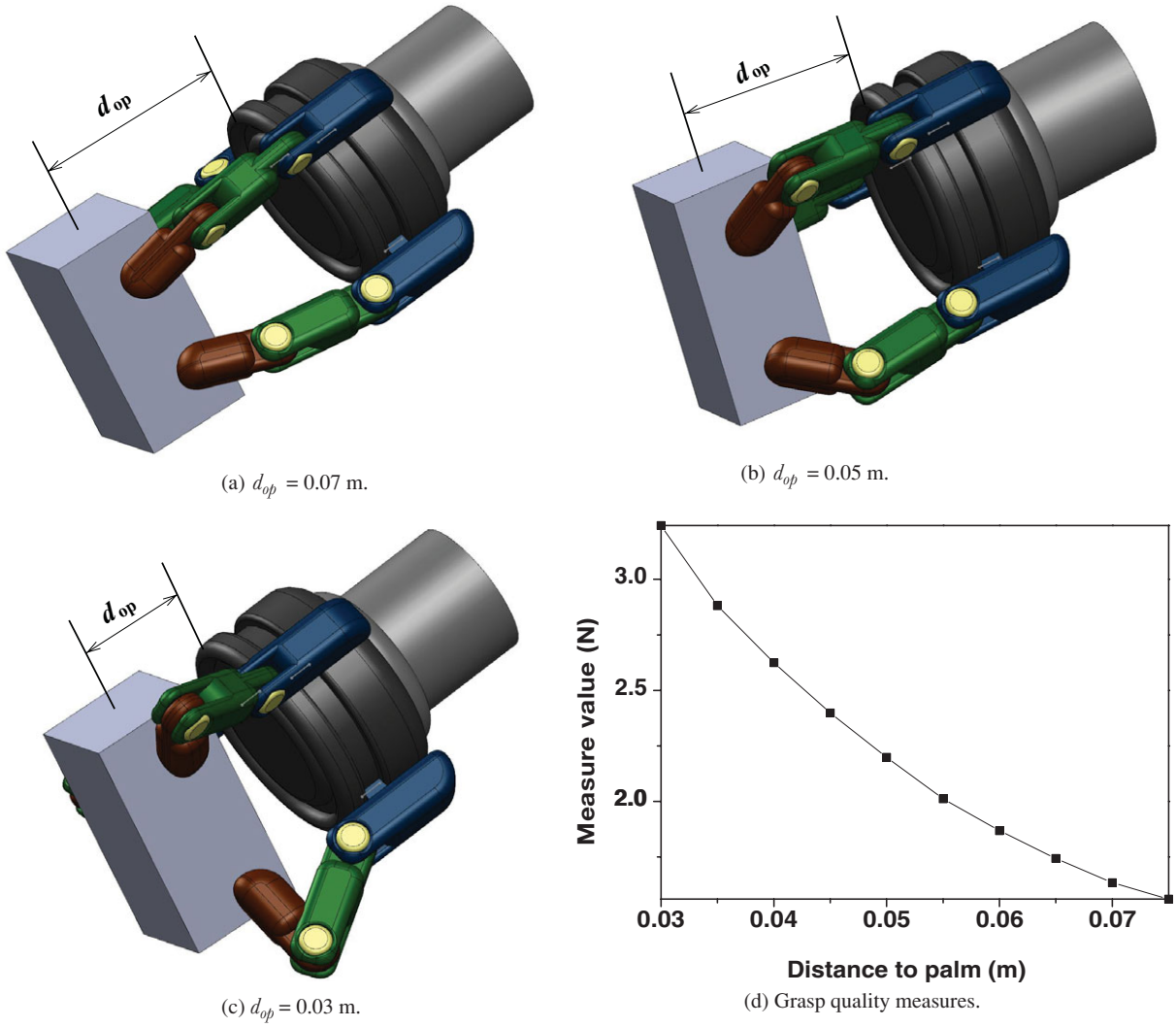


(a) $d_{op}$ = 0.07 m.

(b) $d_{op}$ = 0.05 m.

(c) $d_{op}$ = 0.03 m.

(d) Grasp quality measures.

Fig. 15. (Colour online) Effect of finger configurations to the grasp quality measure.

Development Program for Robot Specialists of the Ministry of Knowledge Economy.

## References


1. N. S. Pollard, "Closure and quality equivalence for efficient synthesis of grasps from examples," *Int. J. Robot. Res.* **23**, 595–613 (2004).
2. M. Hershkovitz and M.Teboulle, "Sensitivity analysis for a class of robotic grasping quality functionals," *Robotica* **16**, 227–235 (1998).
3. C. Borst, M. Fischer and G. Hirzinger, "Grasp planning: how to choose a suitable task wrench space," *Proc. IEEE Int. Conf. Robot. Autom.* **1**, 319–325 (2004).
4. M. Strandberg and B. Wahlberg, "A method for grasp evaluation based on disturbance force rejection," *IEEE Trans. Robot.* **22**(3), 461–469 (2006).
5. V.-D. Nguyen, "*The Synthesis of Stable Force-Closure Grasps*," Technical Report 905, Massachusetts Institute of Technology, Cambridge, MA (1986).
6. B. Mishra, J. T. Schwartz and M. Sharir, "On the existence and synthesis of multifinger positive grasp," *Algorithmica* **2**(4), 541–558 (1987).
7. J. Ponce and V. Faverjon, "On computing three-finger force-closure grasps of polygonal objects," *IEEE Trans. Robot. Autom.* **11**(6), 868–881 (1995).
8. D. Kirkpatrick, B. Mishra and C.-K. Yap, "Quantitative Steinitz's Theorems with Applications to Multifingered Grasping," *Proceedings of the ACM Symposium on Theory of Computing* (1990) pp. 341–351.
9. C. Ferrarari and J. F. Canny, "Planning optimal grasps," *Proc. IEEE Int. Conf. Robot. Autom.* **3**, 2290–2295 (1992).
10. R. M. Murray, Z. Li and S. S. Sastry, *A Mathematical Introduction to Robotic Manipulation*. (CRC, Boca Raton, FL, 1993).
11. Y. H. Liu, "Qualitative test and force optimization of 3D frictional form-closure grasps using linear programming," *IEEE Trans. Robot. Autom.* **15**(1), 163–173 (1999).
12. Z. Li and S. S. Sastry, "Task-oriented optimal grasping by multifingered robot hands," *IEEE J. Robot. Autom.* **4**(1), 32–44 (1988).
13. R. Haschke, J. Steil, I. Steuwer and H. Ritter, "Task-oriented Quality Measures for Dextrous Grasping," *Proceedings of the IEEE International Symposium on Computational Intelligence in Robotics and Automation* (2005), pp. 689–694.
14. J. Cornelia and R. Suarez, "Efficient determination of four-point form-closure optimal constraints of polygonal objects," *IEEE Trans. Autom. Sci. Eng.* **6**(1), 121–130 (2009).


https://doi.org/10.1017/S0263574711000713 Published online by Cambridge University Press

15. Y. Yokokohji, J. San Martin and M. Fujiwara, "Dynamic manipulability of multifingered grasping," *IEEE Trans. Robot.* **25**(4), 947–954 (2009).
16. S. Salimi and G. M. Bone, "Kinematic enveloping grasp planning method for robotic dexterous hands and three-dimensional objects," *Robotica* **26**, 331–344 (2008).
17. S. Arimoto, R. Ozawa and M. Yoshida, "Two-Dimensional Stable blind Grasping under the Gravity Effect," *Proceedings of IEEE International Conference on Robotics and Automation* (2005) pp. 1196–1202.
18. K. Nishimura and K. Ohnishi, "Gravity Estimation and Compensation of Grasped Object for Bilateral Teleoperation," *IEEE International Workshop on Advanced Motion Control* (2006) pp. 72–77.
19. D. Prattichizzo, J. Aslisbury and A. Bicchi, "Contact and Grasp Robustness Measures: Analysis and Experiments," *Proceedings of Symposium on Experimental Robotics* (1995) pp. 1–6.
20. M. A. Roa and R. Suarez, "Computation of independent contact regions for grasping 3D objects," *IEEE Trans. Robot. Autom.* **25**(4), 839–850 (2009).
21. R. Platt, A. Fagg and R. Grupen, "Null-space grasp control: Theory and experiments," *IEEE Trans. Robot.* **26**, 282–295 (2010).
22. X. Zhu and J. Wang, "Synthesis of force-closure grasps on 3D objects based on the q distance," *IEEE Trans. Robot. Autom.* **19**(4), 669–679 (2003).
23. H. Jeong, J. Park, J. Cheong and F. C. Park, "Grasp planning for three-fingerd robot hands using taxonomy-based preformed grasp and object primitives," *J. Korea Robot. Soc.* **3**, 123–130 (2008).

https://doi.org/10.1017/S0263574711000713 Published online by Cambridge University Press